EXPERIMENTAL AND NUMERICAL DETERMINATION OF CRITICAL FORCES FOR PERFORATED THIN WALLED BARS

A. Piotrowski [1)] M. Gajewski [2)] C. Ajdukiewicz [3)] Ł. Kowalewski [4)] S. Jemioło [5)]

[1)] MSc, Faculty of Civil Engineering, Warsaw University of Technology, POLAND, *a.piotrowski@il.pw.edu.pl*

[2)] PhD, Faculty of Civil Engineering, Warsaw University of Technology, POLAND, *m.gajewski@il.pw.edu.pl*

[3)] PhD, Faculty of Civil Engineering, Warsaw University of Technology, POLAND, *c.ajdukiewicz@il.pw.edu.pl*

[4)] MSc, Faculty of Civil Engineering, Warsaw University of Technology, POLAND, *l.kowalewski@il.pw.edu.pl*

[5)] Prof, Faculty of Civil Engineering, Warsaw University of Technology, POLAND, *s.jemiolo@il.pw.edu.pl*

ABSTRACT: The paper presents results of compression tests of perforated thin walled bars of very low slenderness (varying from 1 to 11). The samples are made from typical low carbon steel and cut from the standard elements of an existing storage system. Because of the elasto-plastic material properties and low slenderness of tested elements, samples are deforming mostly in a local way. Buckling forms are generally similar in all samples, although depending on length several variants differing in the form and direction of movement of the side walls can be observed. The final geometry of the samples (after reaching certain average strain and unloading) is documented by photography and linear dimension measurements giving a good data for calibration of the theory of elasto-plasticity for large deformations. Obtained critical forces are compared with the theoretical results obtained using theory of thin walled beams and finite element solutions presented on LSCE 2016 and LSCE 2017 seminars.

Keywords: experimental results, buckling, critical forces, post-critical modes, thin-walled bars, perforated bars.

1. INTRODUCTION

The paper presents results of compression tests of elements presented in Fig.1. It is the continuation of work presented on XXII and XXIII LSCE conferences: thin-walled bars theory (Refs 6, 9, 10, 11) calculations as well as final element method modelling (Refs 1, 2, 18-20) were presented in Ref. 7, and in Ref. 8 elastic buckling forms were analysed. Some calculations and early experiments were also presented in Ref. 15.
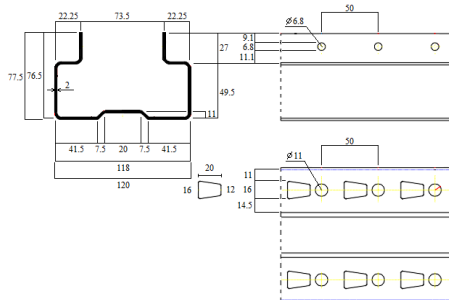

Fig. 1 Characteristic dimensions of tested elements (Ref. 15)

For the need of this paper a wide experimental campaign was conducted. Because of the availability of the equipment we have decided to start with the compression tests of elements of very low slenderness ratio and fixed endings (later on the boundary condition influence is analysed using FEM model).

2. DESCRIPTION OF EXPERIMENTAL TESTS

Elements chosen for testing are presented on Fig.1 and are made from a typical low carbon steel (Ref. 13). Tested samples were 50, 100, 150, 200, 250, 300, 400 and 500 mm long, and were mounted in Instron 8802 universal testing machine using compressing plates with 5 mm fixtures (see Fig. 2). Displacement speed was calculated as 4% of initial length per minute and the end of the test condition was displacement equal to 10% of initial length. Force and displacement were recorded with the testing machine during the test, and after it the chosen permanent displacements were measured manually (see Fig.5).

Fig. 2 Compressing plates with fixtures (Ref. 13)

Whole process was also analysed using ARAMIS digital image correlation system [3]. This part of experiment is not presented in this paper. For more information see Refs 13 and 14.

3. COMPRESSION TEST RESULTS

3.1 Numeration of the samples

Samples were cut from several elements, and although they should be identical, in reality some differences can be seen in the obtained results. From each element 2 sets of samples were obtained. The pairs are: (0.x and 1.x), (2.x and 3.x.1), (3.x.2 and 3.x.3) and (3.x.4 and 3.x.5), where x is the initial length of the sample in centimetres. There are some exceptions to this rule: samples 3.5.1 and 3.15.2 are additional samples created from leftovers of material, and other samples in these two series have their numbers changed because of that (for example, sample that should be named 3.5.1 becomes 3.5.2, 3.5.2 becomes 3.5.3 and so on). Samples 3.10.1, 3.50.2 and 3.50.3 were cut improperly.

3.2 Equilibrium paths

Equilibrium paths obtained during the experiments are shown in Fig.3. They are presented without any processing, especially initial fitting stages are not cut from the graphs.
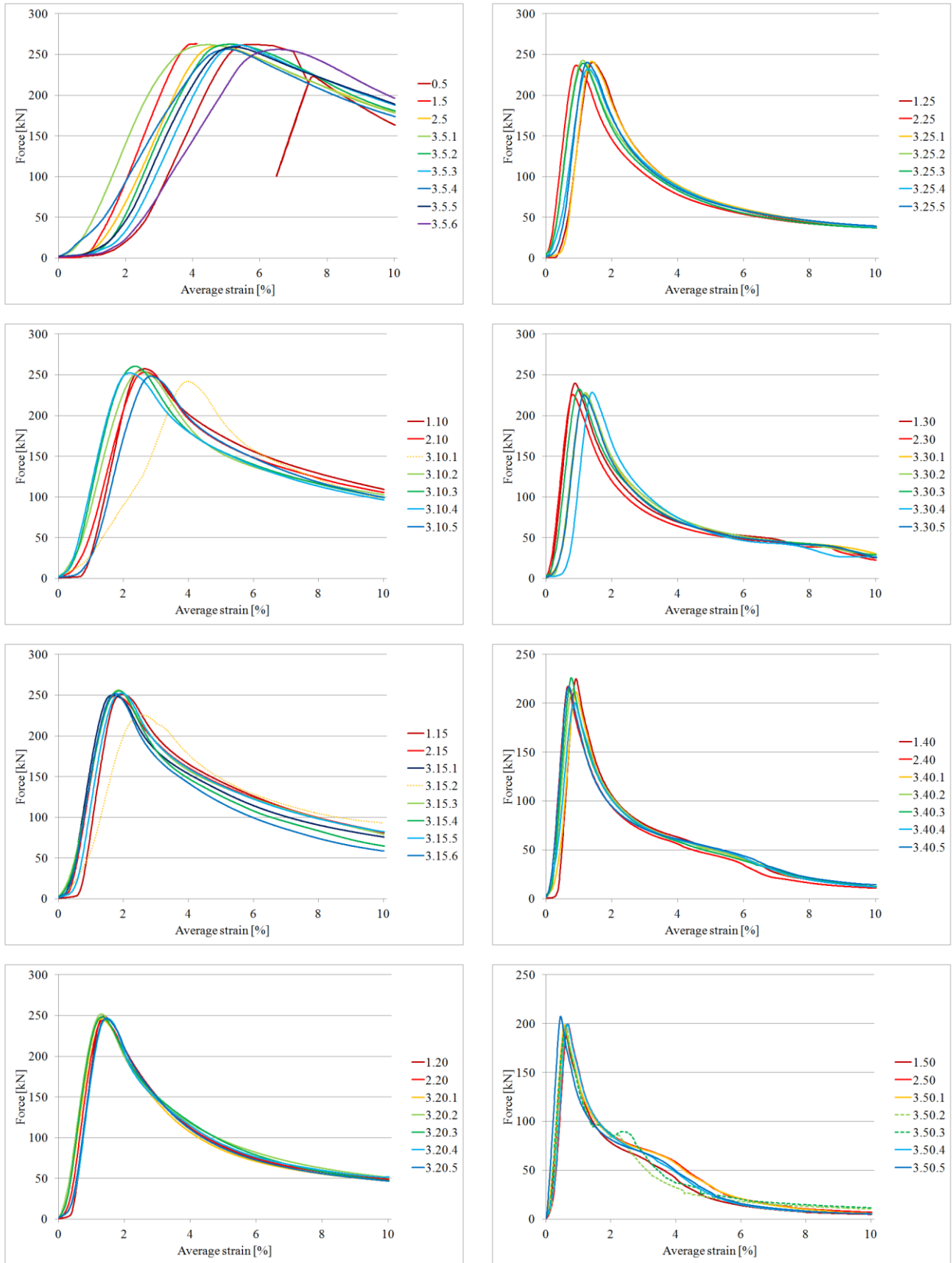
Fig. 3 Equilibrium paths for tested elements of lengths of 5, 10, 15, 20, 25, 30, 40 and 50 cm

3.3 Critical force as the function of slenderness

From results presented in section 3.2 critical loads were determined. In Fig.4 they are presented as the function of slenderness. Points marked with X blue markers are correct values, points marked with red crosses are incorrect values, point marked with square was calculated as force

corresponding to plasticity limit, and the green line is the overall results approximation with the second degree polynomial.
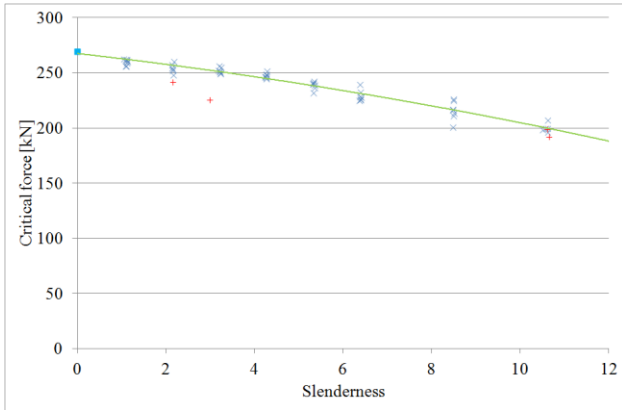

Fig. 4 Critical force as the function of slenderness

3.4 Permanent deformation measurements

Before the test specimen's initial length l_0 was measured. After the test destroyed specimens were measured according to the Fig.5. As it can be seen, selected measurements were: length (measured independently on front and back side of the sample) - l_1 and l_2, distance between flanges in the buckling point - d, distance between the buckling point and the end (always the same) of sample - e and permanent deflection - f. Results of these measurements are written in the Table 1. Because of the differences in buckling forms of samples of different lengths, additional clarifications are given at the end of the table.

Fig. 5 Permanent deformation measurements (Ref. 13)

Table 1. Permanent deformation measurements

no.	λ	l_0 [mm]	l_1 [mm]	l_2 [mm]	d [mm]	e [mm]	f [mm]
0.5	1.118	52.8	49.9	49.8	82	25.8	15.1
2.5	1.131	53.4	50.2	49.9	69.3	12.6	13.9
3.5.1	1.086	51.3	47.5	47.5	69.7	22.6	14.4
3.5.2	1.048	49.5	46.3	46.1	56.2	19.8	14.7
3.5.3	1.114	52.6	49.6	49.4	56.1	16.9	14.0
3.5.4	1.101	52.0	48.4	48.1	54.1	15.6	13.6
3.5.5	1.118	52.8	49.6	49.4	54.4	11.2	13.6
3.5.6	1.084	51.2	48.1	47.9	56.6	18.1	14.2
av.5	1.100	52.0	48.7	48.5	62.3	17.8	14.2
1.10	2.139	101	92.8	91.9	67.5	38.3	26.5
2.10	2.154	101.7	93.7	83.1	34.5	44.7	25.3
3.10.1	2.143	101.2	93.4	81.3	30.5	38.5	22.2
3.10.2	2.132	100.7	92.0	90.3	47.4	41.0	25.7
3.10.3	2.175	102.7	94.0	83.4	45.3	42.8	27.1
3.10.4	2.156	101.8	92.9	80.1	41.4	44.0	25.2
3.10.5	2.162	102.1	93.7	81.6	36.2	38.2	23.5
av.10	2.152	101.6	93.2	84.5	43.3	41.1	25.1
3.15.2	2.982	141	131	132	104	23.7	29.0
av.14	2.982	141	131	132	104	23.7	29.0
1.15	3.219	152	137	140	109	79.0	35.9
2.15	3.221	152	137	139	111	69.2	35.1
3.15.1	3.221	152	139	139	74.3	75.5	29.1
3.15.3	3.193	151	137	138	104	70.2	32.8
3.15.4	3.236	153	140	126	20.5	79.8	28.5
3.15.5	3.179	150	137	137	102	64.8	31.4
3.15.6	3.215	152	139	126	16.9	82.2	27.3
av.15	3.212	152	138	135	76.8	74.4	31.4
1.20	4.257	201	179	181	151	82.9	48.5
2.20	4.267	202	178	181	150	86.8	47.3
3.20.1	4.263	201	179	180	153	89.0	47.9
3.20.2	4.278	202	178	182	145	87.8	47.4
3.20.3	4.259	201	178	181	147	93.0	46.9
3.20.4	4.252	201	183	177	98.1	86.4	37.2
3.20.5	4.240	200	179	179	152	85.8	47.8
av.20	4.259	201	179	180	142	87.4	46.1

no.	λ	l_0 [mm]	l_1 [mm]	l_2 [mm]	d [mm]	e [mm]	f [mm]
1.25	5.315	251	226	226	184	121	55.8
2.25	5.356	253	227	224	181	127	58.8
3.25.1	5.322	251	225	226	177	125	56.9
3.25.2	5.341	252	226	225	180	118	56.1
3.25.3	5.360	253	227	224	182	116	56.6
3.25.4	5.328	252	225	224	180	126	56.9
3.25.5	5.322	251	223	225	178	129	57.3
av.25	5.335	252	226	225	180	123	56.9
1.30	6.374	301	260	277	171	118	73.9
2.30	6.391	302	263	275	176	163	74.9
3.30.1	6.389	302	268	275	177	128	70.9
3.30.2	6.406	303	266	279	170	146	72.6
3.30.3	6.383	301	264	277	172	142	73.2
3.30.4	6.372	301	262	279	164	140	74.3
3.30.5	6.368	301	263	275	175	150	72.1
av.30	6.383	301	264	277	172	141	73.1
1.40	8.492	401	347	372	147	187	103
2.40	8.479	400	352	375	146	187	108
3.40.1	8.494	401	352	375	151	176	105
3.40.2	8.509	402	340	371	151	183	106
3.40.3	8.492	401	338	371	149	182	107
3.40.4	8.479	400	337	371	162	202	106
3.40.5	8.471	400	350	373	161	213	106
av.40	8.488	401	345	373	152	190	106
1.50	10.61	501	427	466	180	217	138
2.50	10.61	501	436	469	165	270	133
3.50.1	10.50	496	427	462	170	243	142
3.50.2	10.59	500	465	420	0.00	219	-77.4
3.50.3	10.63	502	466	421	0.00	230	-78.9
3.50.4	10.57	499	443	469	177	212	131
3.50.5	10.61	501	413	462	174	243	137
av.50	10.58	500	429	466	173	237	136
	10.61	501	466	421	0.00	225	-78.2
	10.59	500	427	466	124	233	75.0
	10.59	500	427	466	124	233	107

AD d:
Symmetric – both sides outwards.
Symmetric – both sides outwards – the material ruptured at the measurement site.
Symmetric – both sides inwards.
Asymmetric – both sides in one direction.
Asymmetric – one side S-shaped, second side inwards – measurement between closest points.
Asymmetric – one side S-shaped, second side outwards – measurement between furthest points.
Asymmetric – both sides S-shaped – measurement between furthest points.
AD l_1, l_2, d and f: buckling form forced by fine trimming and polishing the ends of the sample .
AD averages: from all , *from all shorter/longer l's* , <u>from absolute values</u> , from not forced , from forced .
AD l_0: not precise cutting (differences of about 2 mm between different corners of the sample) .

3.5 Photographs of the samples after unloading

Because of limited length of the paper only selected photographs are shown below. Figs 6-8 present samples of three different lengths: 5cm samples are generally buckling inwards, 25cm samples are generally buckling outwards, and 15 cm samples are the border between two buckling forms.

Fig. 6 Samples with initial length equal to 5 cm.

Fig. 7 Samples with initial length equal to 15 cm
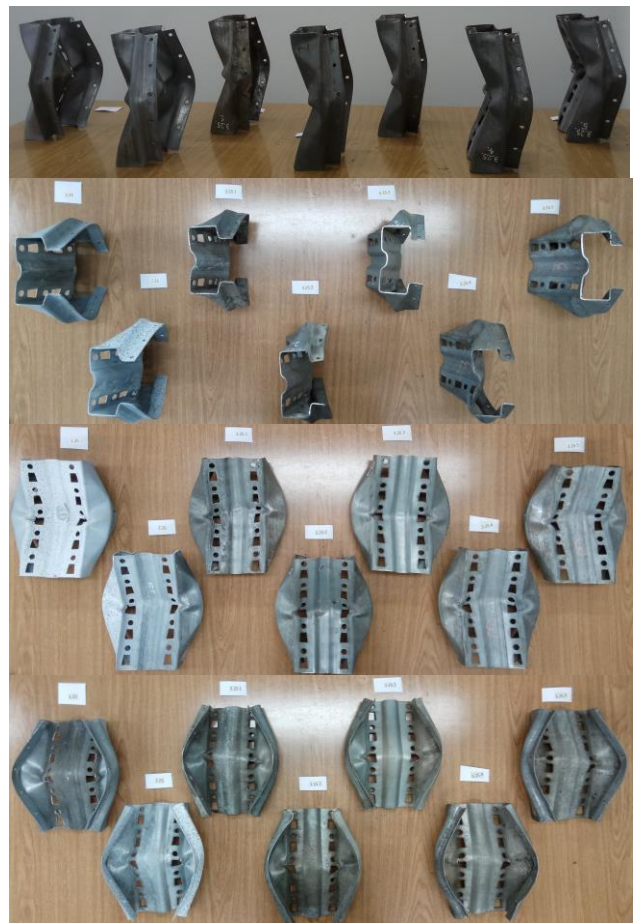

Fig. 8 Samples with initial length equal to 20 cm.

Fig. 9 Samples with initial length equal to 50 cm.

In Fig. 9 two buckling forms observed in the 50 cm samples can be seen: first one with flanges going outwards and second one with flanges going inwards. First one is the normal buckling form of samples of this length, second one was forced by grinding the ends of the samples. It is

interesting, that the maximum forces obtained from grinded samples are not distinctly different from the normal ones.

4. NUMERICAL AND ANALYTICAL RESULTS

Theoretical solutions of the problem were presented in Refs 7, 8, 15. Two main methods were used. The first one was finite element method modeling using shell elements, elasto-plastic material (Ref. 5) and nonlinear procedures. Several variants of this method were used. For the second approach the thin-walled bar theory for elastic buckling of long bars and Johnson-Ostenfeld approximation for plastic buckling of short bars altogether with some ideas from standards (Refs 4, 16, 17) were used. The most important results acquired with both methods are presented in Fig.10.
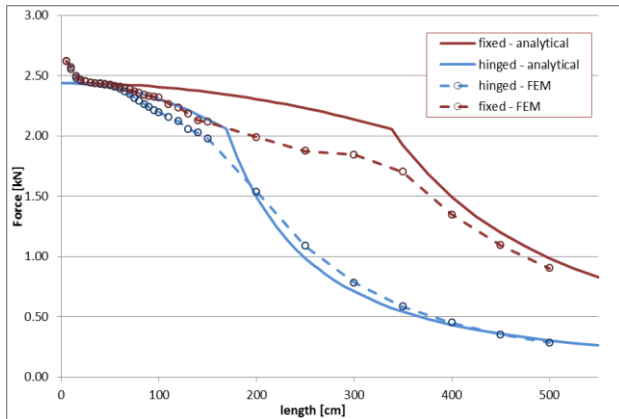

Fig. 10 The comparison of the FEM calculation results to analytical solutions derived with application of thin-walled bar theory (Ref. 7)

5. RESULTS ANALYSIS

In Fig.11 the experimental results on the critical force (maximum points on the equilibrium paths shown in Fig.3) are presented in the form of "x" markers. On that basis the green curve being a second degree polynomial approximation of obtained results is also plotted. In the same graph also the numerical results obtained with application of FEM and shell modelling for two different types of boundary conditions (fixed and hinged, see Fig.10 and Refs 7, 15 for boundary conditions modelling details) are shown (dashed lines with the circles: blue – hinged and dark red – fixed). The blue and dark red continuous lines also visible in the graph represent the analytical approximations based on thin-walled bars theory and Johnson-Ostenfeld curves. Because of very low slenderness, the difference between hinged and fixed boundary conditions in the analytical approach is very small. From obvious reasons presented analytical approach is also quite inaccurate for very short elements. It can be also observed, that finite element method solution for fixed boundary conditions describes the actual experimental results pretty well up to about 20cm of length, but it fails to correctly describe it for longer elements. There are two possible reasons of that fact. Firstly, for longer elements the assumption, that the tested elements have ideally fixed ends, becomes less reasonable.

However, that reason only is clearly insufficient – the experimental results for samples longer than 25cm are lower than the results calculated for hinged boundary conditions. In this situation the geometry imperfections seem to be the most important reason behind the low maximum force values obtained from experiment.

In case of FEM modelling of the analysed compression tests the observed failure mechanisms are predicted with good accuracy. Some examples of failure mechanisms predicted with FEM application in the form of Huber-Mises stress intensities contour plots on the deformed unloaded sample are shown in Figs 12 and 13. In both cases (initial length of the sample equal to 50 and 100 cm) the influence of the boundary conditions is shown. What is more in case of the sample 50 cm long with boundary conditions named as "hinged" the predicted failure mechanism is very similar to one characterized before and shown in Fig. 9 as an exceptional one (the cross section walls after crossing maximum point are rotating in each other direction).
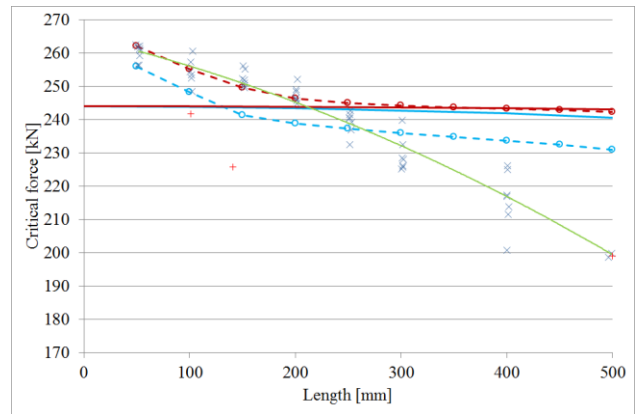

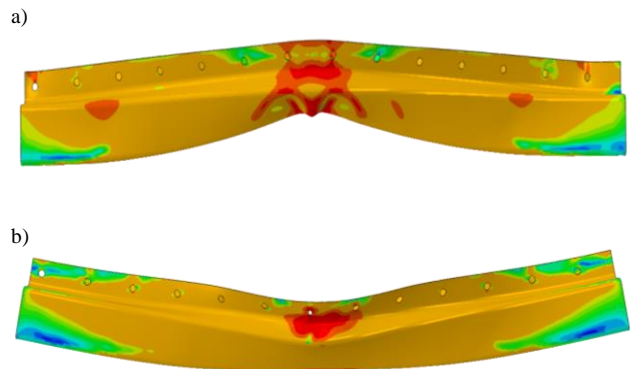Fig. 11 Theoretical and experimental results comparison

Fig. 12 Exemplary failure mechanisms predicted with FEM application (contour plots of Huber-Mises stress intensities on the deformed unloaded sample) for 50 cm length sample obtained with different boundary conditions: a) fixed, b) hinged (cf. with Fig. 9)
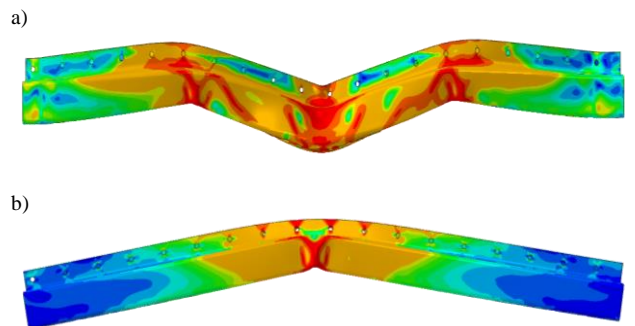

Fig. 13 Exemplary failure mechanisms predicted with FEM application (contour plots of Huber-Mises stress intensities on the deformed unloaded sample) for 100 cm length sample obtained with different boundary conditions: a) fixed, b) hinged

6. CONCLUSIONS

On the basis of the experimental test results presented in Fig.3 it is possible to conclude, that in case of higher slenderness ratio the repeatability of the test is quite good (with respect to the maximum force value and overall equilibrium path). Having in mind that all analyzed samples are rather of a low slenderness value the sample behavior is determined not only by its geometry and elastic material property but also by plasticity properties (Ref. 6). The characteristic failure mechanisms are observed (see Fig. 7, 8 and 9) almost always in the same spatial form. The only difference, that can be observed between samples of different lengths is the direction of movement of flanges. In the elements shorter than 15cm they are moving inwards, in the longer ones outwards and elements, that are 15cm long, can buckle in both ways (and also some mixed variants). What is even more interesting, even after crossing the maximum point in the equilibrium

path (critical force value) the overall answers of the compressed samples are mostly the same (for the chosen slenderness ratio). Only in case of fine trimming and polishing the ends of the longest sample (50cm) a different failure mechanism is manifesting on the equilibrium path (compare Fig. 3 for 50cm samples 3.50.2 and 3.50.3). In those cases the failure mechanisms are shown in Fig.9: in the middle part of the compressed element the web is bended outwards and the flanges are rotating in each other direction after crossing maximum point, while in most of the other cases the web was moving inwards and flanges were moving outwards.

The presented in the Table 1 results on permanent deformation of the elements released after the compression test, may be treated as a data for verification of large deformation shell theories for elasto-plastic materials. Such theories are well developed for the needs of the modelling of cold forming technological processes for thin walled bars.

In Fig.11, the experimental results are shown against the numerical results, obtained with application of FEM program ABAQUS with shell modelling of the compressed element. It can be seen, that the experimental results are laying alongside numerical results obtained for fixed boundary conditions only for the shortest elements. Because of the less significant meaning of the fixture shown on Fig.2 (and resulting from that weakening of boundary conditions) and growing role of imperfections, the longer elements are weaker than the numerical predictions. Important role of geometry imperfections in thin-walled bars is discussed for example in Ref. 12. It seems that for acquiring better compatibility of numerical and experimental results, three measures should be taken: firstly, joints should be used between the testing machine and compression plates, to ensure hinged boundary conditions and uniform pressure at the ends of the samples; secondly, the calculations should describe boundary conditions more precisely; and thirdly, imperfections should be taken into consideration. The tests will be continued in the future.

REFERENCES

1. ABAQUS/Standard User's manual, ver. 6.11. Dassault Systèmes, SIMULIA 2011.

2. ABAQUS Theory Manual, ver. 6.11. Dassault Systèmes, SIMULIA 2011.

3. Aramis v6 User Manual, GOM mbh (2008)

4. Bródka J., Broniewicz M., Giżejowski M.: Kształtowniki gięte. Poradnik Projektanta. PWT Rzeszów 2006.

5. Jemioło S., Gajewski M.: Hyperelasto-plasticity. Warsaw University of Technology Publishing House, Warsaw 2014 (in Polish).

6. Kotełko M., Nośność i mechanizmy zniszczenia konstrukcji cienkościennych, W N-T, Warszawa 2011.

7. Kowalewski Ł., Piotrowski A., Gajewski M., Jemioło S.: FEM application for determination of post-critical deformation modes of perforated thin-walled bars, Monograph from Scientific Seminar Organized by Polish Chapters of International Association for Shell and Spatial Structures, University of Warmia and Mazury, Faculty of Geodesy, Geospatial and Civil Engineering, XXII LSCE –2016, Olsztyn, pp. 27-30, 2016.

8. Kowalewski Ł., Piotrowski A., Gajewski M., Jemioło S.: Determination of critical forces with corresponding deformation modes for perforated thin-walled bars, Monograph from Scientific Seminar Organized by Polish Chapters of International Association for Shell and Spatial Structures, University Science and Technology, Faculty of Civil Engineering, Architecture and Environmental Engineering, XXIII LSCE –2017, Bydgoszcz, pp. 14-17, 2017.

9. Mutermilch J., Kociołek A.: Strength and stability of thin-walled bars with open cross-section. Warsaw University of Technology Publishing House, Warsaw 1964 (in Polish).

10. Obrębski J.B.: Thin-walled elastic bars. Warsaw University of Technology Publishing House, Warsaw 1991 (in Polish).

11. Piechnik St., Pręty cienkościenne – otwarte, Wyd. Politechniki Krakowskiej, Kraków 2000 (in Polish).

12. Paczos P., Kasprzak J.: Influence of actual imperfections on the strength and stability of cold-formed thin-walled C-beam. 28th Symposium of Experimental Mechanics of Solids, Jachranka 2018.

13. Piotrowski A., Gajewski M., Ajdukiewicz C.: Application of digital image correlation system for analysis of local plastic instabilities of perforated thin-walled bars. MATEC Web of Conferences, Vol. 196, Article Number: 01032, 2018.

14. Piotrowski A., Gajewski M., Ajdukiewicz C.: Local plastic instabilities of perforated thin-walled bars – FEM modelling and DIC verification. 28th Symposium of Experimental Mechanics of Solids, Jachranka 2018.

15. Piotrowski A., Kowalewski Ł., Szczerba R., Gajewski M., Jemioło S.: Buckling resistance assessment of thin-walled open section element under pure compression. MATEC Web of Conferences, Vol. 86, Article Number: 01021, 2016.

16. PN-EN 1993-1-3: 2008 Eurocode 3 – General rules - Supplementary rules for cold-formed members and sheeting. (Polish Standardization Committee).

17. PN-80/B-3200 Steel Structures – Designing and static calculations (Polish Standardization Committee).

18. Rakowski G., Kacprzyk Z.: Finite element method in structural mechanics, Warsaw University of Technology Publishing House, Warsaw 2016 (in Polish).

19. Zienkiewicz O.C., Taylor R.L.: The finite element method for solid and structural mechanics, Sixth edition, Elsevier Butterworth Heinemann, 2005.

20. Zienkiewicz O.C., Taylor R.L., Zhu J.Z.: The finite element method – Its basis & fundamentals, Sixth edition, Elsevier Butterworth Heinemann, 2005.